ESOMAT 2009, 06022 (2009)
DOI:10.1051/esomat/200906022

Effect of thermomechanical training on the transformation temperatures and properties of NiTi melt-spun ribbons

K. Mehrabi[1a], M. Bruncko[1,2], A. C. Kneissl[1]

[1] Department of Physical Metallurgy and Materials Testing, University of Leoben, Austria
[2] Faculty of Mechanical Engineering, University of Maribor, Slovenia

Abstract. The present work aims to study the influence of thermomechanical training and two-way shape memory effect (TWSME) on the transformation behaviour of Ni-50.3 at. % Ti melt-spun ribbons by differential scanning calorimetry (DSC). The results showed that the transformation temperatures decrease with an increase in the number of thermal cycles. The austenitic transformation remains a one-stage transformation, while the martensitic transformation changes to a two-stage transformation. These changes are due to the appearance of an intermediate phase which was stabilized probably by the accumulation of defects introduced by thermomechanical training. The phase that is present after training was studied by X-ray diffraction and transmission electron microscopy.

1. Introduction

NiTi alloys are the most technological important shape memory alloys (SMAs) in a wide range of applications, often as actuators and sensors, since with a shape memory element a pre-determined response can be obtained very easily by thermal or electric stimulus. Especially the possibility to realize even complicated movements with an element of simple design and compact size makes shape memory actuators very attractive [1,2]. There is also a trend to very small-dimensioned shape memory elements which could be used as microactuators. In these applications the NiTi components often experience repeated transformation cycles, either under external load or free of constraint. One critical concern in the development of such devices is the stability of the shape memory properties. Obviously, unstable transformation cycles with associated difficulties in accurate predictions of materials behaviour and device design in the presence of these instabilities are not desirable for actuator applications.

From the several modes of shape memory effect, the two-way shape memory effect (TWSME) is the most suitable to apply in actuators since no resetting force has to be considered in design. However, it is not inherent to SMAs, but can be exhibited after specific repetitive thermomechanical treatments known as training procedures through which SMAs memorize the low temperature shape. To date, more than 20 different training procedures have been investigated and published in efforts to develop a TWSME of both high magnitude and stability which have the common feature that external applied stress should be used, such as tension, compression, torsion or bending. There are some training methods without applied load, which induce internal stress by quenching, ion irradiation or external magnetic fields [3]. It is generally perceived that the development of TWSME originates from the preferential nucleation and growth of martensite variants that are essentially guided by the internal stress field [4]. During the training process, the resulting stress field assists the formation and growth of preferentially oriented martensite variants when the martensitic transformation proceeds in a specimen on cooling [5].

It is well known that in NiTi alloys a change of the transformation temperatures and appearance of an intermediate phase can take place due to thermomechanical training, thermal cycling, aging at an appropriate temperature, and other processing techniques [6]. The precipitation of an intermediate phase in NiTi brings about an excellent shape memory property with a small hysteresis. Therefore, the presence of the intermediate phase is useful in engineering fields [7].

For practical applications, control of transformation characteristics is quite important. Therefore, the main object of this paper was to study the influence of training parameters on the efficiency, transformation temperatures, and intermediate phase of Ni-50.3 at. % Ti melt-spun ribbons.

[a] e-mail: kambiz.mehrabi@unileoben.ac.at

2. Experimental Procedure

The NiTi alloy ingots were prepared by vacuum arc-melting on a water-cooled copper hearth in a reduced Ar atmosphere. To ensure homogeneity, arc-melting was repeated three times for each alloy.
The melt-spun ribbons were produced under a 200 mbar He atmosphere using quartz-glass crucibles with a nozzle diameter of 0.9 mm, coated internally with Y_2O_3. By applying an Ar overpressure of ~90 mbar within the crucible, the melt was ejected onto the surface of a polished Cu wheel (200 mm diameter) having a circumferential wheel speed of 5 to 30 ms^{-1}. The distance between the nozzle and the wheel surface was 2 mm.
For inducing a two-way shape memory effect there are several methods; one is based on temperature cycling under constant stress which is an effective method for introducing a TWSME and allows a good control of the training parameters [8, 9], however is limited to linear shape changes.
In this study, a bending training method was applied to NiTi ribbons which consists of several thermal cycles under constant bending strain followed by load-free thermal cycling.
The bending deformation strain (ε_d) of the outer surface of the specimen was calculated using the equation $\varepsilon_d = d/(D+d)$, where d is the ribbon thickness and D is the diameter of the constrained circle.
The one-way shape recovery strain (ε_{1w}), two-way shape memory strain (ε_{2w}) and plastic deformation (η_p) were measured by the values of $\varepsilon_{1w}=[(\theta_0-\theta_1)/\theta_0]\times\varepsilon_d$, $\varepsilon_{2w}=[(\theta_2-\theta_1)/\theta_0]\times\varepsilon_d$ and $\eta_p=\theta_1/\theta_0$, respectively, where the angle $\theta_0=180°$ and the deformation angles θ_1 and θ_2 are indicated in Fig. 1. The value of spontaneous shape change during heating and cooling was recorded by photographs. During the constrained training and subsequent free thermal cycling, the temperature was changed from room temperature (RT) to 250 °C. While the TWSME was executed several hundred times, the changes in the deformation behaviour and the stability of the effect were continuously observed.

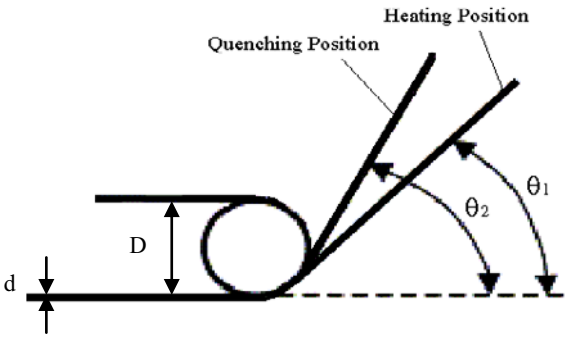

Fig. 1. Schematic illustration for bending examination of TWSME.

Specimens for metallographic investigation were cut from the longitudinal cross sections of melt-spun ribbons. They were ground on SiC paper to a final mesh size of 2400 and polished. The samples were etched in a solution containing $HF–HNO_3–CH_3COOH$ = 2:4:5 and studied by optical microscopy. For TEM experiments, thin discs (3 mm in diameter) were mechanically ground to a thickness of 60 μm and polished in an electrolyte consisting of 20% sulphuric acid and 80% methanol at 273–278 °K using a twin jet electro-polisher, according to [10]. Ion-milling was then performed on the samples for 30 minutes. The energy of the Ar+ ions was 3.6 keV, the angle to the surface of the specimen was ±4°, and the specimen was kept at a rotation rate of 3 rpm during ion-milling. Conventional TEM studies were performed on a Philips CM12 at an acceleration voltage of 120 kV.
The phase transformation temperatures of trained ribbons were measured using a Mettler DSC 821e device (Mettler Toledo GmbH, Schwerzenbach, CH). Thermograms were recorded under static air from –40 to 180 °C at a heating/cooling rate of 10 K min^{-1}. A circular sample disc was cut with a punch (5 mg), put in a 20 μl aluminium pan, and sealed with a perforated lid. The crystallographic structure was determined using Bragg-Brentano X-ray diffraction with Cu-K_α radiation at room temperature. Tensile specimens with gauge size of 25–30 mm in length, 2 mm in width, and about 80 μm in thickness were cut from the melt-spun ribbons and tested at room temperature on a universal mechanical testing machine, designed for small samples.

3. Results and discussion

Some researchers (e.g. [11–13]) consider it necessary that after rapid cooling a heat treatment has to be performed in order to achieve shape memory effects. The reason for this is that in their work higher cooling rates and, therefore, partially amorphous structures were obtained which have to be annealed for crystallization. We have performed our experiments on three different melt-spinning devices and on a splat-cooling device and always obtained martensitic samples which exhibited a fully crystallized microstructure and shape memory effects immediately after processing. Figure 2 shows the martensitic microstructure of a ribbon produced by

melt-spinning at a medium wheel speed (15 ms^{-1}). It was observed that the increase in the wheel speed from 5 to 30 ms^{-1} results in a decrease in the ribbon thickness from ~100 to ~30 μm. As the increase in the wheel speed leads to a reduced ribbon thickness, the cooling rate increases and therefore the martensitic substructure gets finer.

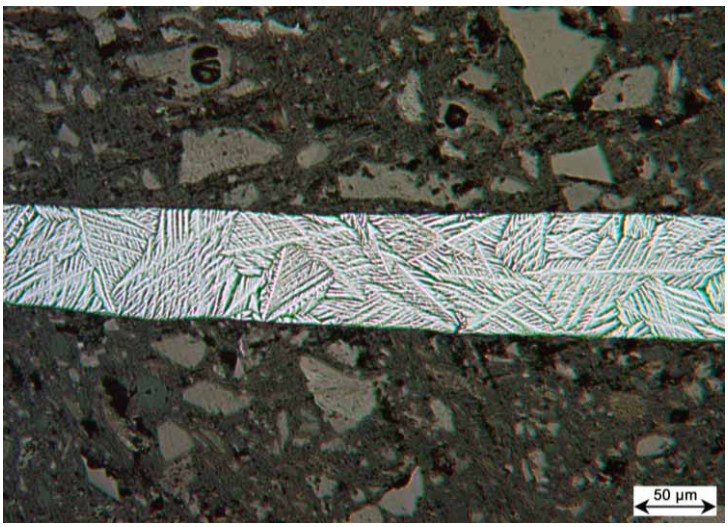

Fig. 2. Martensite structure of a NiTi ribbon at a wheel speed of 15 m/s.

3.1. TWSME induced by thermomechanical training

In this method, pieces of NiTi ribbons (~50 mm long and 2 mm wide) were bent to a small radius (about 0.9 mm) with a surface strain of 8 % and cycled through the transformation range several times (3–10 times) in a constrained condition (the angle θ = 180°). The resulting two-way effect increases with increasing number of constrained thermal cycles in the early stage and then decreases after reaching a maximum point, while with increasing number of constrained thermal cycles, the plastic deformation increases strongly and therefore the shape recovery ratio reduces. This fact suggests that an appropriate density of slip defects is effective for the improvement of the TWSME while an excessive density of defects and plastic deformation reduce the TWSME. The two-way effects were not very high; however, after several hundred free thermal cycles (not constrained) the two-way effect became larger with higher shape recovery and finally stabilized. It is not yet known exactly why this interesting functional behaviour occurs but it seems that shape memory samples cannot only be trained under the usual constrained conditions but also to a certain extent by free thermal cycles. The results of the constrained training treatment and effect of free thermal cycles are summarized in Table 1 and Table 2, ε_{1w}, ε_{2w} and η_p denoting the size of one-way shape memory effect, two-way shape memory effect and plastic deformation, respectively.

Table 1. Resulting one-way and two-way shape memory effects after constrained training.

Training Number	One-way Effect, ε_{1w} (%)	Two-way Effect, ε_{2w} (%)	Plastic Deformation, η_p (%)
1	6.66	0.31	16.66
3	5.78	0.58	27.77
5	3.20	0.98	60
10	1.86	0.31	76.66

Table 2. Influence of free thermal cycles on shape memory effects after 5 constrained training cycles.

Training Number	One-way Effect, ε_{1w} (%)	Two-way Effect, ε_{2w} (%)	Plastic Deformation, η_p (%)
1	3.20	0.98	60
10	4.49	1.11	43.89
100	5.51	1.56	31.11
200	6.18	1.69	22.77
300	6.89	1.78	13.88
400	7.56	1.82	5.55
500	7.73	1.78	3.33

3.2. Effect of training on precipitation

TEM examinations were performed on as-spun and trained ribbons. Figure 3a displays a fine martensitic structure (B19′ phase) with nano-sized twin boundaries in the as-spun NiTi ribbons. After 5 constrained training cycles and 500 free thermal cycles, many fine spherical particles were observed by TEM as shown in Fig. 3b. By selected area diffraction these particles (indicated by arrows) could be identified as $NiTi_2$. The size of the precipitates was estimated to be in the order of several hundred nanometres. Results from EDX analysis also indicate that the spherical particles are $NiTi_2$, as shown in Table 3.

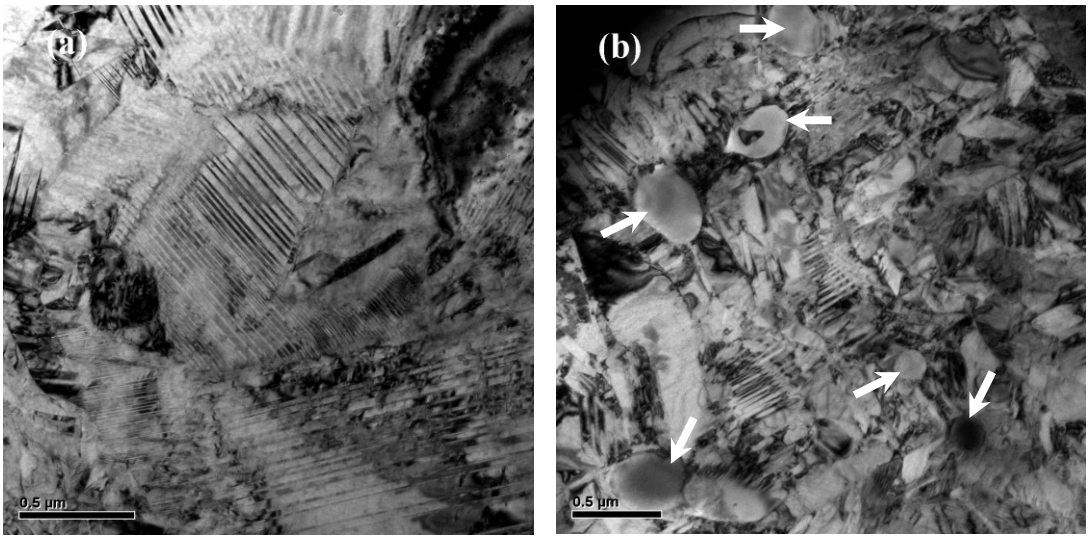

Fig. 3. TEM micrograph of the B19′ microstructure in a melt-spun NiTi ribbon: (a) before training, (b) after training.

Table 3. EDX results from the matrix and $NiTi_2$ particles.

	Ti (at. %)	Ni (at. %)
NiTi-matrix	51.1	48.9
$NiTi_2$ particles	66.5	33.5

3.3. DSC results

The transformation behaviour with increasing number of free thermal cycles after one constrained training cycle is shown in Fig. 4. The height of the peak of austenitic phase transformation (endothermic behaviour) increases and the transformation temperatures decrease slightly. The decrease in austenitic transformation temperatures and the increase in the height of the austenitic peak indicate an easier transformation from martensite to austenite which may be related to the presence of a dislocation structure that serves as a network of nucleation sites for the austenite phase [14]. The exothermic behaviour (during cooling) of the transformation shows that an intermediate phase (which is $NiTi_2$) appears during thermal cycles. The peaks shift gradually to the lower temperature side, and the temperature region of the intermediate phase is expanded. It is thought that the accumulation of lattice defects introduced by thermomechanical training and thermal cycles leads to the stabilization of the intermediate phase.

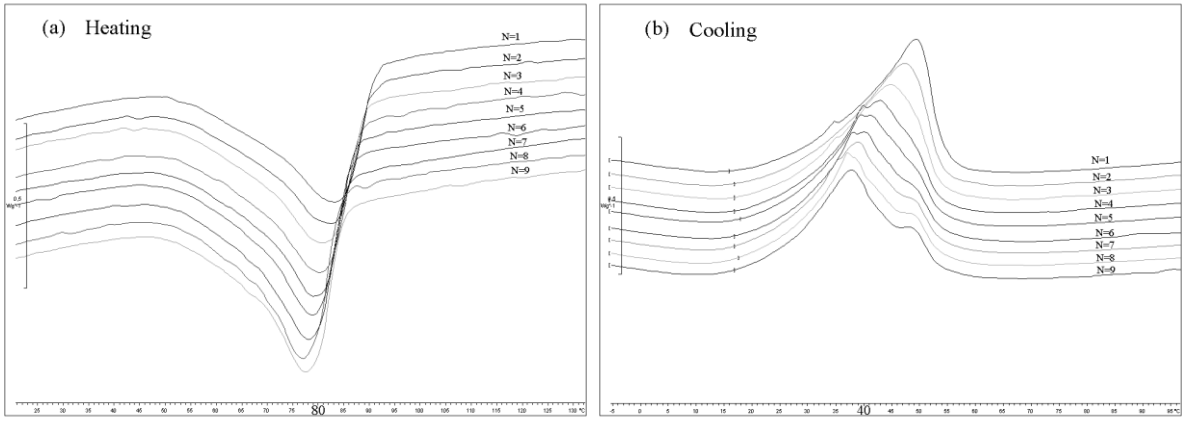

Fig. 4. DSC results from NiTi ribbons with different numbers of thermal cycles: (a) heating, (b) cooling.

Figure 5 shows an XRD pattern from the melt-spun ribbons before and after thermomechanical training. As shown in the figure, all peaks in the trace before training belong to the B19´ martensite, while after training an intermediate phase is detected which has been identified as $NiTi_2$ precipitates.

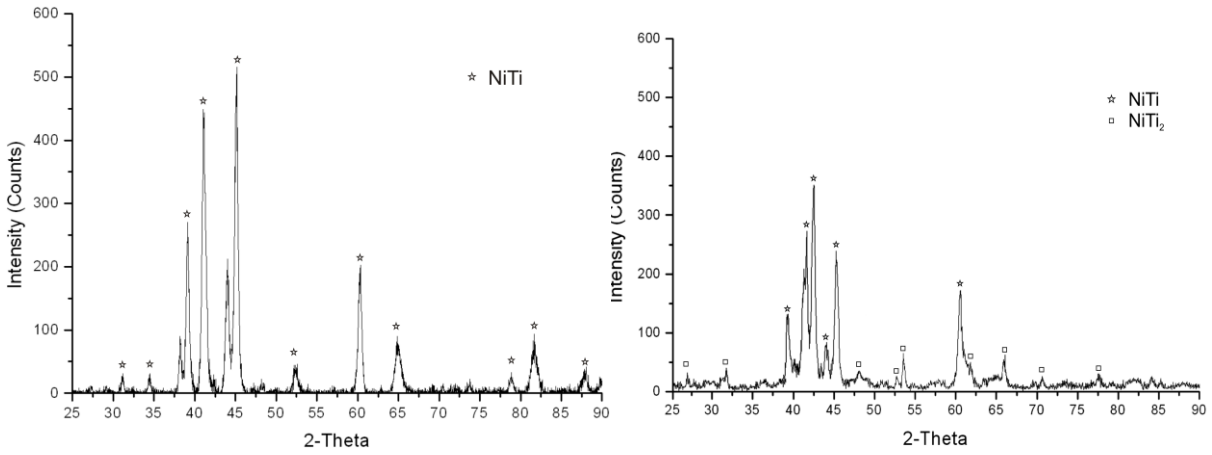

Fig. 5. XRD pattern of a NiTi ribbon, B19´ phase: (a) before training, (b) after training.

3.4. Tensile test

Tensile tests of melt-spun ribbons fabricated at various wheel speeds show clearly the martensitic plateau even without subsequent heat treatment (e.g. Fig. 6a). The pseudoplastic deformation reaches about 4 % strain before plastic deformation occurs. The samples fracture at a strain of about 7 %. The results of the tensile test performed after thermomechanical training is shown in Fig. 6b. It clearly shows a higher strength than the ribbons without training. This is caused probably by the $NiTi_2$ precipitates and a higher dislocation density. During these tests we have unloaded and reloaded 5 times. The deviation between the unloading path and reloading path is very small. This experimental result reveals that the deformation of the specimen is fully pseudoplastic and that there is no austenite phase and pseudoelastic effect at all.

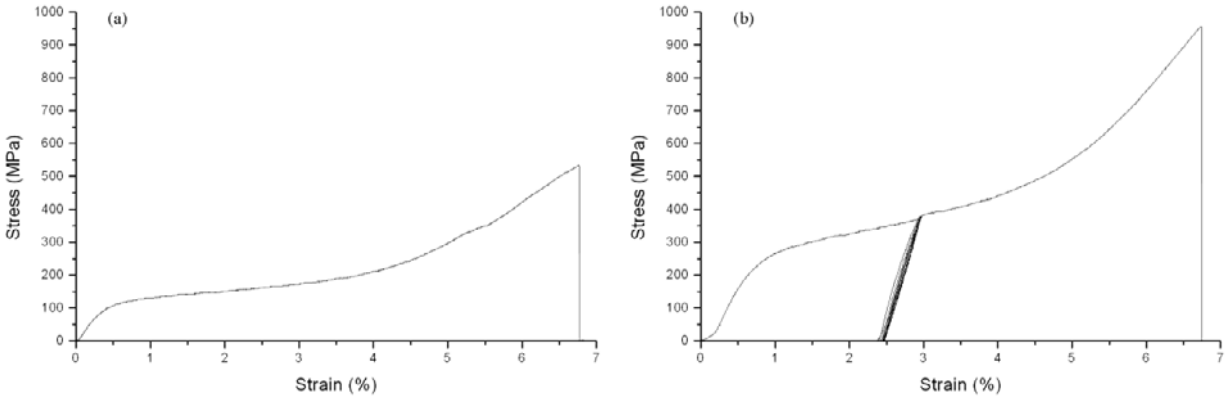

Fig. 6. Stress-strain curve from the melt-spun ribbon: (a) before training, (b) after training.

4. Conclusions

(1) After melt-spinning the samples consist of a martensite phase and show a shape memory effect without subsequent heat treatment.
(2) The bending training method is an effective method to induce a TWSME in the NiTi ribbons. The NiTi ribbons could be trained by a combination of constrained and free thermal cycles and show two-way shape memory effects sufficient for technical long-term applications.
(3) The resulting TWSME increases with increasing number of constrained thermal cycles in the early stages and then decreases after reaching a maximum point, while with an increasing number of

constrained thermal cycles the plastic deformation increases strongly and therefore the shape recovery ratio reduces.

(4) After several hundred free thermal cycles (not constrained) the two-way effect became larger with higher shape recovery and finally stabilized.
(5) The microstructure of melt-spun ribbons after thermomechanical training consists of two phases, martensite B19′ and a $NiTi_2$ precipitates.
(6) The height of the austenitic peak (endothermic behaviour) increases and the transformation temperatures decrease slightly with an increase in the number of cycles. The exothermic behaviour of the transformation shows that an intermediate phase ($NiTi_2$) appears during thermal cycles, which is stabilized probably by the accumulation of defects introduced by thermal cycles.
(7) After training, many fine $NiTi_2$ spherical particles were observed by TEM and therefore, the trained ribbons show higher strength than ribbons without training. Since these ribbons have good mechanical properties (strength and ductility) they seem very suitable for future microactuator applications.

Acknowledgment

We are grateful to Prof. Dr. G. Dehm for enabling us to use the TEM at the Erich Schmid Institute of Materials Science, Austrian Academy of Sciences, Leoben.

References

[1] Y. Liu, J. Laeng, T.V. Chin, T.H. Nam, Mater. Sci. Eng. A 435–436 (2006) 251–257.
[2] P. Ochin, V. Kolomytsev, A. Pasko, P. Vermaut, F. Prima, R. Portier, Mater. Sci. Eng. A 438–440 (2006) 630–633.
[3] X. M. Zhang, J. Fernandez, J.M. Guilemany, Mater. Sci. Eng. A 438–440 (2006) 431-435.
[4] K. Wada, Y. Liu, Mater. Sci. Eng. A 481–482 (2008) 166–169.
[5] Ch. Y. Chang, D. Vokoun, Ch. T. Hu, Metall. Mater. Trans. A 32 (2001) 1629.
[6] Y. Motemani, M. Nili-Ahmadabadi, M.J. Tan, M. Bornapour, Sh. Rayagan, J. Alloys Compd. 469 (2009) 164–168.
[7] H. Matsumoto, J. Alloys Compd. 350 (2003) 213–217.
[8] L. Contardo, G. Guenin: Acta Metall. Mater. 38 (1990) 1267.
[9] Y. Liu, P.G. McCormick: Acta Metall. Mater. 38 (1990) 1321.
[10] L.J. Chiang, C.H. Li, Y.F. Hsu, W.H. Wang, J. Alloys Compd. 462 (2008) 47-51.
[11] R.D. Jean, J.C. Tsai: Scripta Metall. Mater. 30 (1994) 1027.
[12] Y. Liu, P.G. McCormick: Proc. ICOMAT-92, Monterrey Inst. of Advanced Studies (1993) 923.
[13] Y. Liu, J. Humbeeck, R. Stalmans, L. Delaey: J. Alloys Compd. 247 (1997) 115.
[14] S. Turenne, S. Prokoshkin, V. Brailovski and N. Sacepe, Can. Metall. Q. 39 (2000), pp. 217–224.